

Tyrosine promotes anthocyanin biosynthesis in pansy (*Viola × wittrockiana*) by inducing ABA synthesis

Authors

Zheng Cui, Jia Gu, Jie Li, Anjin Zhao, Yingge Fu, ..., Ting Peng*, Jian Wang*

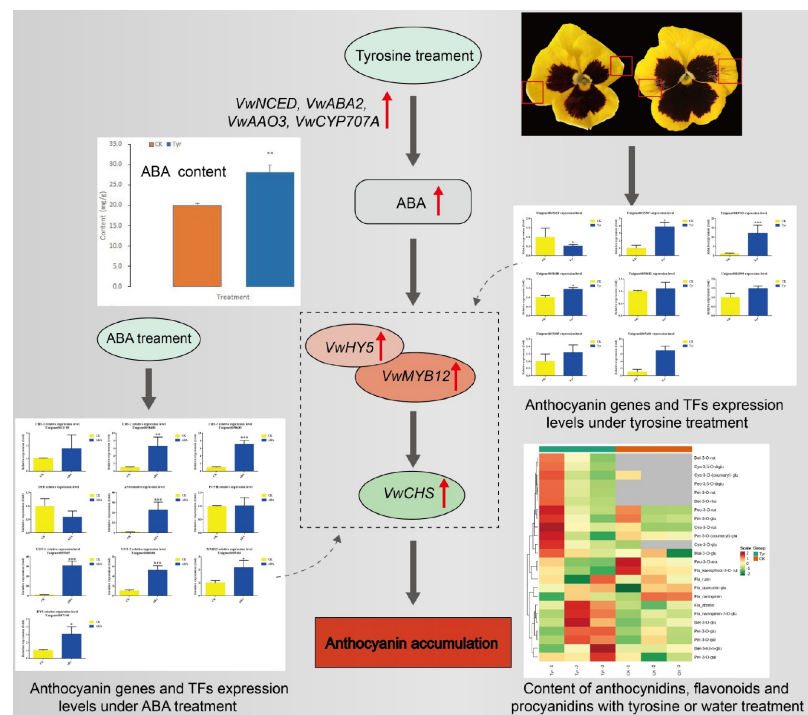
Correspondences

nancybin1987923@163.com;
wjhainu@hainanu.edu.cn

In Brief

This study establishes a possible novel regulatory network for anthocyanin biosynthesis, tyrosine induces ABA synthesis and thereby promotes anthocyanin biosynthesis in pansy petals, and the results can reveal the possible mechanism that tyrosine effects in pansy, and may provide a novel insight to the anthocyanins generation in plants.

Graphical abstract




Highlights

- Tyrosine promoting the anthocyanin biosynthesis in pansy.
- Tyrosine decarboxylase gene of pansy (*VwTYDC*) expressed differently in blotches and non-blotched areas of petals.
- Tyrosine induced ABA synthesis and promoted anthocyanin biosynthesis in pansy petals.

Citation: Cui Z, Gu J, Li J, Zhao A, Fu Y, et al. 2022. Tyrosine promotes anthocyanin biosynthesis in pansy (*Viola × wittrockiana*) by inducing ABA synthesis. *Tropical Plants* 1:9 <https://doi.org/10.48130/TP-2022-0009>

Tyrosine promotes anthocyanin biosynthesis in pansy (*Viola × wittrockiana*) by inducing ABA synthesis

Zheng Cui^{1#}, Jia Gu^{1#}, Jie Li¹, Anjin Zhao¹, Yingge Fu¹, Tongxin Wang¹, Tingge Li¹, Xueqing Li¹, Yuhui Sheng^{1,3}, Ying Zhao¹, Xiqiang Song¹, Yang Zhou¹, Ting Peng^{2*}, and Jian Wang^{1*} 

¹ Key Laboratory of Genetics and Germplasm Innovation of Tropical Forest Trees and Ornamental Plants, Ministry of Education, Key Laboratory of Germplasm Resources Biology of Tropical Special Ornamental Plants of Hainan, College of Forestry, Hainan University, Haikou, Hainan 570228, China

² Guizhou University, Guiyang, Guizhou 550025, China

³ Hengxing University, Qingdao, Shandong 266100, China

These authors contributed equally: Zheng Cui, Jia Gu

* Corresponding authors, E-mail: nancybin1987923@163.com; wjhainu@hainanu.edu.cn

Abstract

Viola × wittrockiana (pansy) is an important ornamental plant, particularly during winter and spring. In previous studies, we found that the tyrosine decarboxylase gene of pansy (*VwTYDC*) was expressed differently in blotched and non-blotched areas of pansy petals, suggesting that tyrosine may have a role in anthocyanin biosynthesis. In this study, we found that virus-induced gene silencing of *VwTYDC* caused an accumulation of pink pigmentation in pansy petals. Likewise, exogenous tyrosine treatment (TYRT) induced the formation of black stripes in non-blotched petal areas. Metabolome analysis indicated that the contents of two anthocyanins, cyanidin-3-O-glucoside and cyanidin-3-O-rutinoside, increased significantly in the TYRT areas. RT-qPCR results revealed that the anthocyanin-related genes *VwHCT*, *VwC3'H*, *VwCHS*, and *VwUGT* were upregulated in the same areas. Transcriptome analysis revealed that four genes involved in the abscisic acid (ABA) biosynthesis pathway (*VwNCED*, *VwABA2*, *VwAAO3*, and *VwCYP707A*) were significantly upregulated in the same TYRT areas. ABA content was measured by ESI-HPLC-MS/MS, and ABA content was significantly higher in TYRT areas than in control areas. In addition, when exogenous ABA was spread onto non-blotched petal areas, anthocyanin biosynthesis genes were upregulated just as with tyrosine. Thus, transcriptome and metabolite analyses revealed a possible novel regulatory network for anthocyanin biosynthesis in which tyrosine induces ABA synthesis and ABA then promotes anthocyanin biosynthesis in pansy petals.

Citation: Cui Z, Gu J, Li J, Zhao A, Fu Y, et al. 2022. Tyrosine promotes anthocyanin biosynthesis in pansy (*Viola × wittrockiana*) by inducing ABA synthesis. *Tropical Plants* 1:9 <https://doi.org/10.48130/TP-2022-0009>

INTRODUCTION

Pansy (*Viola × wittrockiana* Gams.), an important biennial plant in the Violaceae, is widely grown as a commercial flower for its white, yellow, orange, red, blue, and purple flowers in winter and spring. In some cultivars, anthocyanins accumulate at the base of the petals to generate variegated patches or blotches^[1]. For example, purple blotches on the white flowers of 'Mont Blanc' mainly contain cyanidin-p-coumarylglycoside, and purple blotches on the yellow flowers of 'Rhinegold' contain mainly delphinidin-3:5-p-coumaryl glucorhamnoside^[2]. In our previous research, we showed that blotch formation was caused primarily by accumulation of cyanidin and delphinidin.

Anthocyanins are major pigments from the flavonoid family that are responsible for flower color, pollinator attraction, and UV protection^[3,4], and the pathways of flavonoid and anthocyanin biosynthesis are well understood in most model plants^[5]. They involve a variety of biosynthesis genes, such as phenylalanine ammonia-lyase (PAL), chalcone synthase (CHS), chalcone isomerase (CHI), flavanone 3-hydroxylase (F3H), flavonoid 3'-hydroxylase (F3'H), flavonoid 3',5'-hydroxylase (F3'5'H), dihydroflavonol 4-reductase (DFR), and anthocyanidin synthase (ANS)^[6]. Almost all anthocyanidins undergo several modifications, including glycosylation, acylation, and methylation, which are catalyzed by glycosyltransferases (GTs),

acyltransferases (ATs), and methyl transferases (MTs), respectively. Together, these genes synergistically regulate the biosynthesis of anthocyanins^[7].

The transcriptional regulation of flavonoid and anthocyanin biosynthesis genes by transcription factor (TF) complexes of R2R3-MYB, bHLH, and WD40 family members has been widely demonstrated^[5]. For example, *AtMYB11*, *AtMYB12*, and *AtMYB111* of *Arabidopsis thaliana* target similar genes in the flavonoid biosynthesis pathway, including *CHS*, *CHI*, *F3H*, and *flavonol synthase 1 (FLS1)*^[8]. Likewise, basic region/leucine zipper (bZIP) TFs have equally pivotal and diverse roles in the regulation of anthocyanin biosynthesis. An example is *AtHY5*, which promotes the expression of *AtMYB12* and the accumulation of anthocyanins under light conditions in *Arabidopsis*^[8].

Anthocyanin biosynthesis is typically regulated by specific phytohormones. In previous studies, jasmonic acid^[9], cytokinins^[10], ethylene^[11], brassinosteroids^[12], and abscisic acid^[13] have been shown to promote anthocyanin accumulation by activating the transcription of anthocyanin biosynthesis genes, usually via TFs. In *Lycium*, for example, ABA stimulated transcription of the MYB-bHLH-WD40 (MBW) TF complex to upregulate expression of genes in the flavonoid biosynthetic pathway, thereby promoting anthocyanin production and fruit coloration^[14]. In apple treated with ABA, the

Anthocyanin biosynthesis in pansy

MdbZIP44 TF enhanced the ability of MdMYB1 to bind to the promoters of the anthocyanin biosynthesis genes *MdDFR* and *MdUFGT*^[15].

Tyrosine is an aromatic α -amino acid that contains a phenolic hydroxyl group^[16]. It is also a precursor for the shikimate pathway, which feeds into the anthocyanin pathway when tyrosine ammonia lyase (TAL) is active^[17]. In recent years, tyrosine has been shown to upregulate anthocyanin-positive TFs such as *PAP1*, *PAP2*, and *EGL3* and induce anthocyanin biosynthesis in *Arabidopsis thaliana*^[18]. Recently, we found that tyrosine decarboxylase (TYDC), which catalyzes tyrosine to tyramine, was significantly upregulated in blotched areas relative to non-blotched areas of pansy petals, suggesting that tyrosine may play an important role in anthocyanin biosynthesis. In addition, our research indicated that tyramine might contribute to flower color and blotch formation as a co-pigment of anthocyanins in pansy^[19]. Based on these findings, we speculated that tyrosine might also effect anthocyanin biosynthesis in pansy petals. However, more details are needed to fully understand how tyrosine affects anthocyanin biosynthesis in pansy.

In the present study, we performed virus-induced gene silencing (VIGS) to block the expression of *VwTYDC* and thus increase tyrosine content in order to determine whether this would promote anthocyanidin accumulation in pansy. Anthocyanin-free areas of pansy petals were treated with exogenous tyrosine or water and were then used for transcriptome sequencing, metabolite analysis, gene expression verification, and anthocyanin measurements. The results revealed a possible mechanism by which tyrosine contributes to the formation of pansy petal blotches and provide new insights into the production of anthocyanins in plants.

MATERIALS AND METHODS

Plant materials

Viola × wittrockiana 'Mengdie' (Fig. 1) plants were used as materials and were planted at the horticultural farm of Hainan University (20.03N, 110.19E), in Haikou, Hainan Province, China. The plants were cultivated in 18-cm pots from winter to early spring (November 2019 through March 2020). During the planting period, soil moisture remained above 60%, the average daily temperature was about 20 °C, and the daylength was about 11 h. When the flowers were in full bloom, they were used for VIGS assays and ABA treatments.

Virus-induced gene silencing

The pTRV1 and pTRV2 vectors were used to perform the VIGS assay on blooming pansy flowers. Partial sequences of *VwANS* (300 bp), *VwCHS* (270 bp) and *VwTYDC* (300 bp) were cloned into the pTRV2 vector, with *VwCHS* and *VwANS* serving as positive controls. The primers are shown in Supplemental Table S1. *Agrobacterium* strain GV3101 was transformed with the plasmids, pTRV1, pTRV2, pTRV2-*VwANS*, pTRV2-*VwCHS* and pTRV2-*VwTYDC*, then cultured in liquid YEP medium containing 100 mg/L kanamycin and 20 mg/L rifampicin. All samples were shaken at 28 °C at 250 rpm until the OD₆₀₀ value reached 1.0. The bacterial cultures were then centrifuged, and the supernatants were removed. The residues were resuspended in MMA solution (10 mM MgCl₂·6H₂O, 10 mM 2-[N-morpholino] ethanesulfonic acid [MES], and 148 μ M acetosyringone) and the OD₆₀₀ value was readjusted to 1.0. Each MMA solution

containing pTRV2-*VwCHS*, pTRV2-*VwTYDC*, pTRV2-*VwANS*, or pTRV2 was mixed with MMA solution containing pTRV1 (V/V, 1:1) and incubated in the dark for 2–3 h. The mixed solutions were then injected into the epidermis at the top of the pansy stem, and any phenotypic changes in the petals were observed and photographed over subsequent days.

Tyrosine and ABA treatment of non-blotched areas on pansy petals

Petals of blooming pansy flowers were treated with 3 mM tyrosine (CAS:60-18-4, Sigma, USA). A syringe tip was used to pierce the upper epidermis of non-blotched areas, and tyrosine solution was smeared onto the punctured regions. Plants in the control group were treated with ddH₂O. After 24 h, the treated tissues were collected for anthocyanin analysis and total RNA extraction. All samples were immediately frozen in liquid nitrogen and stored at –80 °C. Treatment with 50 μ M ABA (S-ABA, CAS:14375-45-2, Phyto Technology Laboratories, USA) was similar to the tyrosine treatment, and all treatments had three biological replicates.

Anthocyanin detection

The anthocyanin metabolome of petals treated with tyrosine or ddH₂O was analyzed using a UPLC-ESI-MS/MS system (UPLC, ExionLC™ AD, Sciex; MS, Applied Biosystems 6500 Triple Quadrupole, Sciex). The frozen petals were ground into powder (30 Hz, 1.5 min), and 50 mg of powder was weighed and extracted in 0.5 mL methanol/water/hydrochloric acid (500:500:1, V/V/V). The extract was then vortexed for 5 min, ultrasonicated for 5 min, and centrifuged at 4 °C and 13,000 rpm for 3 min. The residue was re-extracted by repeating the above steps again under the same conditions. The supernatants were collected and filtered through a 0.22- μ m membrane filter (Anpel) before LC-MS/MS analysis with a Waters ACQUITY BEH C18 column (1.7 μ m, 2.1 mm \times 100 mm) and a solvent system of water (0.1% formic acid): methanol (0.1% formic acid). The gradient program was 95:5 V/V at 0 min, 50:50 V/V at 6 min, 5:95 V/V at 12 min, hold for 2 min, 95:5 V/V at 14 min; and hold for 2 min. The flow rate was 0.35 mL/min, the



Fig. 1 Phenotypes of *VwTYDC*-silenced *Viola × wittrockiana*. (a) Blank control; (b) flower phenotype after infection with pTRV2-*VwCHS*; (c) flower phenotype after infection with pTRV2-*VwANS*; (d) flower phenotype after infection with pTRV2-*VwTYDC*.

temperature 40 °C, and the injection volume 2 µL. The ESI source operation parameters were as follows: ion source, ESI+; source temperature, 550 °C; ion spray voltage (IS), 5,500 V; curtain gas (CUR), 35 psi. Anthocyanin contents were detected by MetWare based on the AB Sciex QTRAP 6500 LC-MS/MS platform.

ABA analysis

ABA contents were analyzed using an ESI-HPLC-MS/MS system (HPLC, Agilent 1290; MS/MS, Applied Biosystems 6500 Quadrupole Trap). Frozen petals were ground into powder (30 Hz, 1.5 min), and 1.5 g of powder was weighed and extracted in 0.4 mL isopropanol/water/hydrochloric acid. Then, 8 µL of 1 µg/mL internal standard solution was added, and the mixture was shaken at low temperature for 30 min. Dichloromethane was added, the extract was shaken at low temperature for 30 min and centrifuged at 4 °C and 13,000 rpm for 5 min, and the supernatants were removed. The residual organic phase was dried with nitrogen and reconstituted in methanol. The extract was centrifuged at 4 °C and 13,000 r/min for 10 min. The supernatants were filtered through a 0.22-µm filter membrane and measured by HPLC-MS/MS using a Poroshell 120 SB-C18 column (2.7 µm, 2.1 mm × 150 mm) and a solvent system of (A) methanol (0.1% formic acid) and (B) water (0.1% formic acid). The gradient program was 0–1 min, 20% A; 1–9 min, 20%–80% A; 9–10 min, 80% A; 10–11 min, decrease to 20% A; 11–15 min, 20% A. The injection volume was 2 µL. The ESI source operation parameters were as follows: ion source, ESI+; source temperature, 400 °C; IS, 4,500 V; CUR, 15 psi. Analyst software (Sciex) was used to analyze the ABA data.

RNA extraction, cDNA library construction, and mRNA sequencing

RNA was extracted from the tyrosine- and water-treated areas of pansy petals using a modified TRIzol method. Three biological replicates were used for the analysis. High-quality RNA was used for mRNA sequencing: mRNA was enriched with Oligo(dT) beads, and the enriched mRNA was then broken into short fragments using fragmentation buffer and reverse transcribed into cDNA using random primers. Second-strand cDNA was synthesized using DNA polymerase I, RNase H, dNTP, and buffer. The cDNA fragments were purified with the QiaQuick PCR extraction kit, end repaired, poly(A) tailed, and ligated to Illumina sequencing adapters. The ligation products were selected by agarose gel electrophoresis, PCR amplified, and sequenced using the Illumina HiSeq 4000 platform by Gene Denovo Biotechnology Co. (Guangzhou, China).

mRNA transcriptome data analysis

Sequencing reads were filtered by removing adaptor-contaminated reads, reads with > 10% unknown nucleotides (Ns), and reads with > 40% low-quality (Q-value ≤ 20) bases. The high-quality clean reads were mapped to rRNA to identify residual rRNA reads, and such reads were removed. The remaining high-quality clean reads were mapped to the reference transcriptome using Bowtie 2 with default parameters^[20], and the mapping ratio was calculated. Trinity was used to assemble the clean sequencing data to obtain unigenes^[21].

The gene abundances were calculated and normalized to RPKM (Reads Per Kilobase per Million reads)^[22], and the expression levels of unigenes in the two treatments were calculated. Differentially expressed genes (DEGs) between the tyrosine and ddH₂O treatments were identified and filtered using edgeR

(www.bioconductor.org/packages/release/bioc/-html/edgeR.html) based on $FDR < 0.05$ and $|\log_2FC| > 1$. The DEGs were input to Blast2GO software and in-house perl scripts for gene ontology (GO) term analysis, and KEGG pathways were assigned to the assembled genes using the KEGG Automatic Annotation Server (KAAS, www.genome.jp/kegg/) in order to determine their biological functions, metabolic pathways, and signal transduction pathways. To identify TFs, the assembled transcriptomes were searched against the Plant Transcription Factor Database (<http://planttfdb.cbi.pku.edu.cn>) using hmmsearch v3.0 (<http://hmmer.org>).

The protein functional annotations of unigenes were obtained by performing blastx (www.ncbi.nlm.nih.gov/BLAST) against the NR, Swissprot, KEGG, and COG/KOG annotation databases (E-value < 10⁻⁵). Functions of unigenes that did not receive protein annotations were predicted with ESTScan^[23]. After GO annotation of unigenes with Blast2GO software^[24], WEGO was used to calculate functional classification statistics for all unigenes with GO annotations^[25].

qRT-PCR analyses of mRNA

The RNA samples obtained for transcriptome sequencing were also used for quantitative reverse transcription-polymerase chain reaction (qRT-PCR). Reverse transcription was performed for single-stranded DNA synthesis using the PrimeScript RT reagent Kit with gDNA Eraser (TaKaRa, Shanghai, China) according to the manufacturer's protocol. qRT-PCR was performed with three technical replicates and three biological replicates. The 18S gene was used as an internal control for normalization. qRT-PCR analysis was performed using Luna Universal qPCR Master Mix (New England Biolabs, Ipswich, MA, USA) according to the manufacturer's instructions with denaturation at 95 °C for 60 s and 40 cycles of amplification (95 °C for 15 s, 60 °C for 30 s). Expression levels of the target genes relative to the internal control were calculated using the 2^{-ΔΔCt} method^[26]. The gene-specific primers are shown in Supplemental Table S2.

Transcription factor phylogenetic analyses

Protein sequences of the MYB and bZIP TFs from *Arabidopsis* were obtained from NCBI. The gene sequences of pansy MYBs and bZIPs were obtained from the transcriptome, and their conserved domains were analyzed using SMART software in Genomic mode with default parameters. Phylogenetic trees of the two TF families were constructed using MEGA 5.02 with default parameters.

Statistical analysis

ABA content experiments and qRT-PCR analyses were performed in triplicate. Univariate values were analyzed using ANOVA, and mean values were compared using Duncan's new multiple range test ($P < 0.05$) with SAS software (SAS Institute Inc., Cary, NC, USA).

RESULTS

VIGS verified that tyrosine promotes anthocyanin biosynthesis in pansy petals

VIGS was performed to verify the function of *VwTYDC*. As shown in Fig. 1, there was no change in flower phenotype after injection of the blank control pTRV2 (Fig. 1a), but the blotches disappeared or became smaller when plants were injected with the positive controls pTRV2-*VwANS* and pTRV2-*VwCHS* (Fig. 1b,

Anthocyanin biosynthesis in pansy

c). In the pTRV2-*VwTYDC* treatment, the flower color changed to pink (Fig. 1d), indicating pigment accumulation in petals when *VwTYDC* was silenced.

Phenotypic changes and anthocyanin accumulation of pansy petals treated with exogenous tyrosine

To determine how tyrosine effects anthocyanin accumulation in pansy petals, non-blotched petal areas were treated with exogenous tyrosine. Petal phenotypes were observed after 24 h of treatment with water or tyrosine: there were no obvious changes in the non-blotched areas following water treatment (Fig. 2a), but cyanic stripes appeared in the non-blotched areas of pansy petals following treatment with tyrosine (Fig. 2b).

ESI-HPLC-MS/MS was used to scan for 108 anthocyanidins,

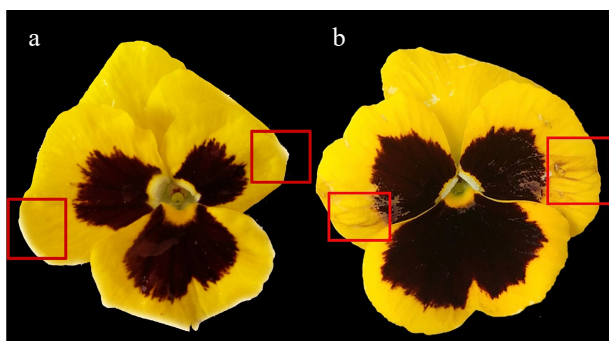


Fig. 2 Effect of tyrosine treatment on non-blotched areas of *Viola x wittrockiana* petals. (a) ddH₂O treatment; (b) tyrosine treatment. The treated areas are marked by a red box.

flavonoids, and procyanidins in the petal areas that received tyrosine or water treatment, and 24 compounds were detected in at least one of the treatments (Supplemental Table S3). The LC-MS/MS data have been uploaded to MetaboLights under number MTBLS3419. The contents of all 24 compounds in different samples were analyzed by hierarchical clustering analysis (Figs 3 & 4). The contents of two metabolites, cyanidin-3-O-glucoside and cyanidin-3-O-rutinoside, differed based on the threshold Fold Change ≥ 2 or Fold Change ≤ 0.5 (Fig. 3). However, if compounds with an expression level of N/A in the CK treatment were included, there were nine differentially abundant anthocyanidins, including cyanidins, delphinidins, petunidins, peonidins and pelargonidins. Among these, cyanidin-3-O-rutinoside showed the highest content of 5.098 ng/g. Delphinidin-3-O-rutinoside, delphinidin-3-O-rhamnoside, cyanidin-3,5-O-diglucoside, petunidin-3-O-rutinoside, peonidin-3,5-O-diglucoside, peonidin-3-O-galactoside, and pelargonidin-3-O-(coumaryl)-glucoside were detected in the tyrosine treatments but not in the water treatments (Fig. 4).

RNA sequencing, gene functional annotation, and classification

Three cDNA libraries were constructed from petals treated with tyrosine, and 57,665,984, 41,950,452 and 49,379,404 high-quality reads were obtained. Three more cDNA libraries were constructed from the control samples, and 52,086,074, 46,811,096, and 48,288,596 high-quality reads were obtained. The final transcriptome assembly contained 90,732 genes with an average length of 735 nt and an N50 of 1,172 nt. The sequencing raw data have been deposited into the NCBI Sequence Read Archive (SRA) under accession number PRJNA754504.

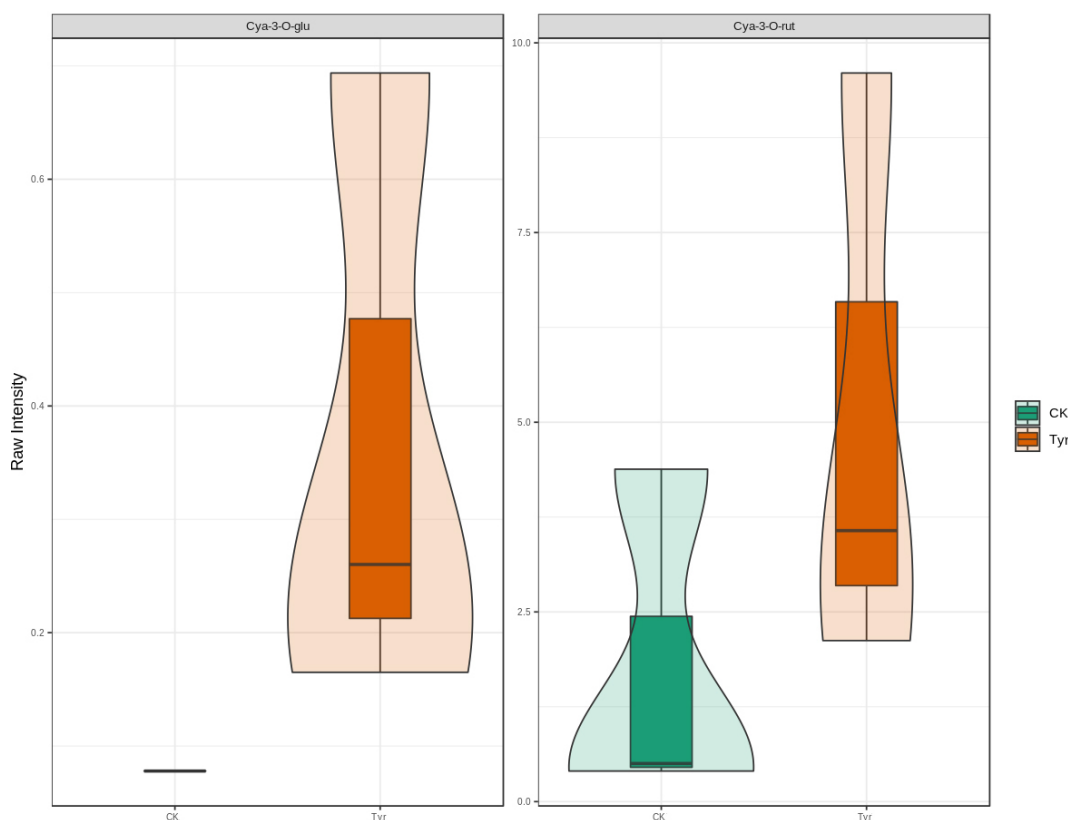


Fig. 3 Violin plot of anthocyanins in petals of *Viola x wittrockiana* treated with tyrosine or ddH₂O. The box in the middle represents the interquartile range. The black horizontal line in the middle is the median, and the outer shape represents the distribution of the data.

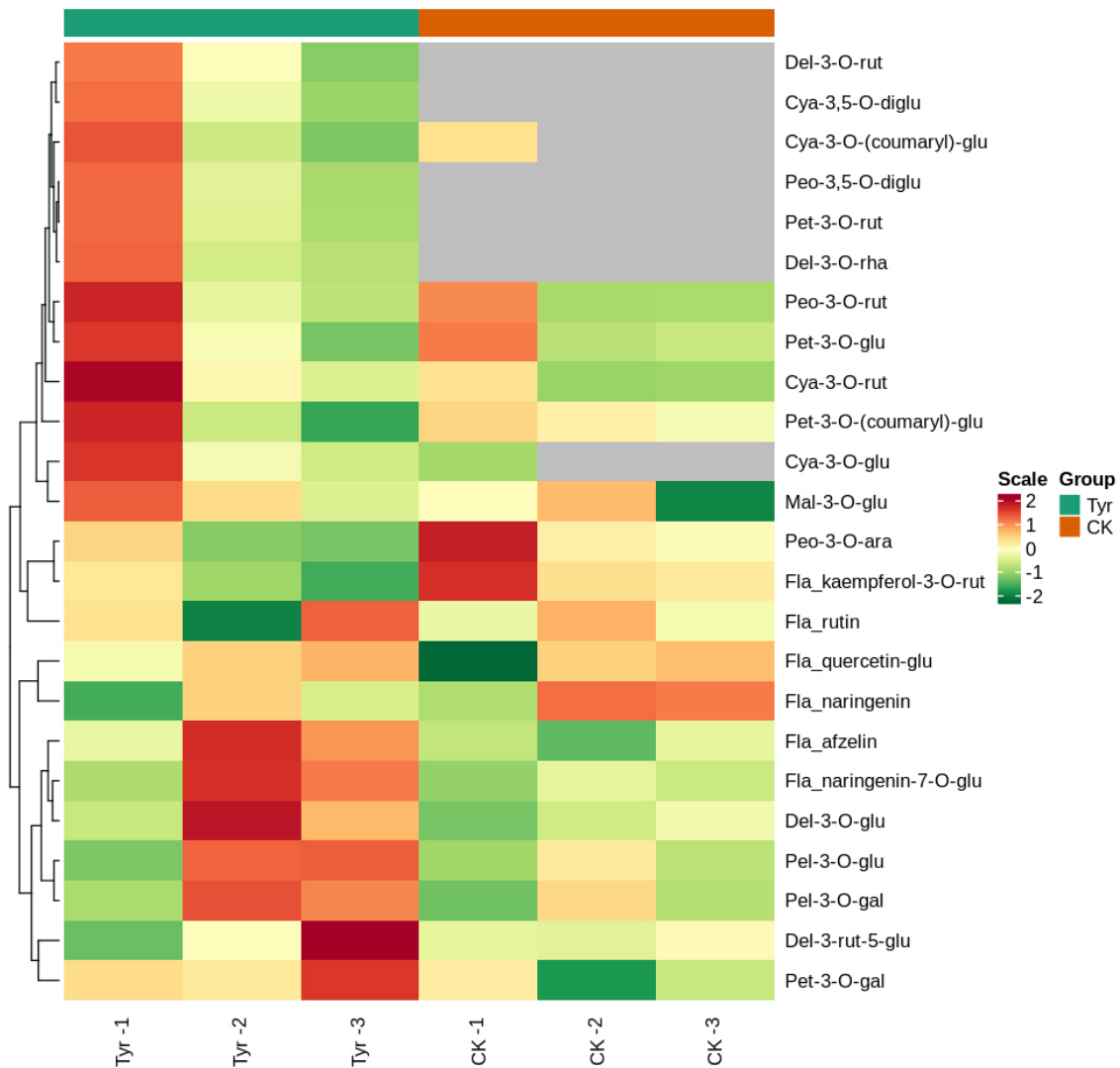


Fig. 4 Heatmap of the contents of the 24 compounds detected in different *Viola × wittrockiana* samples analyzed by hierarchical clustering analysis. The horizontal axis shows the sample information, and the vertical axis shows the metabolite information. The tree on the left of the figure shows the metabolite clustering, and the scale is the metabolite content after standardization. A deeper red color indicates a higher content, and gray indicates that the compound was not detected. Groups indicate the different treatments. CK: ddH₂O treatment; Tyr: tyrosine treatment.

To assign putative functions to the assembled genes, their sequences were searched against public databases; 50,829 genes were annotated by the NR database, and 36,481 genes were annotated by the KOG database. GO annotations (16,976 genes) and KEGG pathway annotations (15,175 genes) were also obtained to gain more insight into the putative gene functions. In the GO analysis, the terms metabolic process, catalytic activity, cellular process, binding, and single-organism process were the top five annotations with the largest number of genes (Supplemental Fig. S1). In the KEGG pathway analysis, the pathways with the greatest unigene enrichment were metabolic pathways (5790, 38.15%), followed by biosynthesis of secondary metabolites (3089, 20.86%), and biosynthesis of antibiotics (1622, 10.69%).

Identification of DEGs related to anthocyanin biosynthesis

A total of 19,438 DEGs were detected between water- and tyrosine-treated areas of pansy petals: 6401 downregulated

and 13,037 upregulated (Supplemental Fig. S2). Among these, 4525 were mapped to 131 KEGG pathways. There were nine DEGs related to anthocyanin biosynthesis in the tyrosine-treated areas, and all but unigene0045619 were upregulated (Table 1). *VwHCT* (unigene0045619, unigene0015507), *VwC3'H* (unigene0083763, unigene0029000), and *VwCHS* (unigene0058680, unigene0058682, unigene0011199) were involved in the flavonoid biosynthesis pathway (ko00941), whereas *VwUGT75C1* (unigene0060888, unigene0055085) was involved in the anthocyanin biosynthesis pathway (ko00942).

Analysis of differentially expressed MYB transcription factors

There were 13 differentially expressed MYB TFs: eight upregulated and five downregulated (Supplemental Table S4). We constructed a phylogenetic tree that included the MYB TFs of *Arabidopsis thaliana* to provide insight into the potential functions of these differentially expressed MYB TFs (Supplemental Fig. S3). We found that unigene0005403 was highly homolo-

Anthocyanin biosynthesis in pansy

gous to the *Arabidopsis* TFs AT5G49330.1, AT2G47460.1, and AT3G62610.1, which encode *AtMYB111*, *AtMYB12*, and *AtMYB11*. A blastx search of the transcriptome data indicated that this unigene was also highly similar to an *MYB12-like* TF gene from *Cicer arietinum* (E-value < 10^{-5}), and we therefore speculated that it was likely to be an *MYB12-like* gene in pansy.

qPCR of key anthocyanin biosynthesis and transcription factor genes

The relative expression levels of 10 DEGs (nine biosynthesis genes and one TF gene) related to the anthocyanin biosynthe-

sis pathway were verified in tyrosine- and ddH₂O-treated petals by qPCR. The expression levels of these DEGs were again promoted by tyrosine, with the exception of unigene0045619 (*HCT-1-like*) (Fig. 5), consistent with the transcriptome sequencing results (Table 1).

Tyrosine upregulates ABA biosynthesis-related genes and promotes ABA production

The transcriptome data revealed that expression levels of some key genes in the ABA biosynthesis pathway were significantly higher in the tyrosine-treated areas than in the H₂O-

Table 1. Putative anthocyanin structural genes that were differentially expressed in response to tyrosine treatment in *Viola × wittrockiana* petals.

Gene ID	Annotation	RPKM (Tyr treatment)	RPKM (H ₂ O treatment)	log ₂ (T/CK)	FDR	Up/Down
unigene0045619	<i>VwHCT</i>	0.54	1.48	-1.45	0.05	Down
unigene0015507	<i>VwHCT</i>	2.31	0.56	2.26	5.35e-12	Up
unigene0083763	<i>VwC3'H</i>	3.60	0.34	3.42	1.18e-28	Up
unigene0029000	<i>VwC3'H</i>	1.80	0.02	6.86	8.38e-15	Up
unigene0058680	<i>VwCHS</i>	213.61	100.30	1.09	4.65e-35	Up
unigene0058682	<i>VwCHS</i>	87.86	42.41	1.05	1.18e-41	Up
unigene0011199	<i>VwCHS</i>	10.51	3.40	1.63	6.24e-33	Up
unigene0060888	<i>VwUGT75C1</i>	13.30	5.71	1.22	2.95e-21	Up
unigene0055085	<i>VwUGT75C1</i>	177.86	66.99	1.41	3.19e-105	Up

VwHCT, shikimate O-hydroxycinnamoyltransferase; *VwC3'H*, coumaroylquinate 3'-monooxygenase; *VwCHS*, chalcone synthase; *VwUGT75C1*, anthocyanidin 3-O-glucoside 5-O-glucosyltransferase.

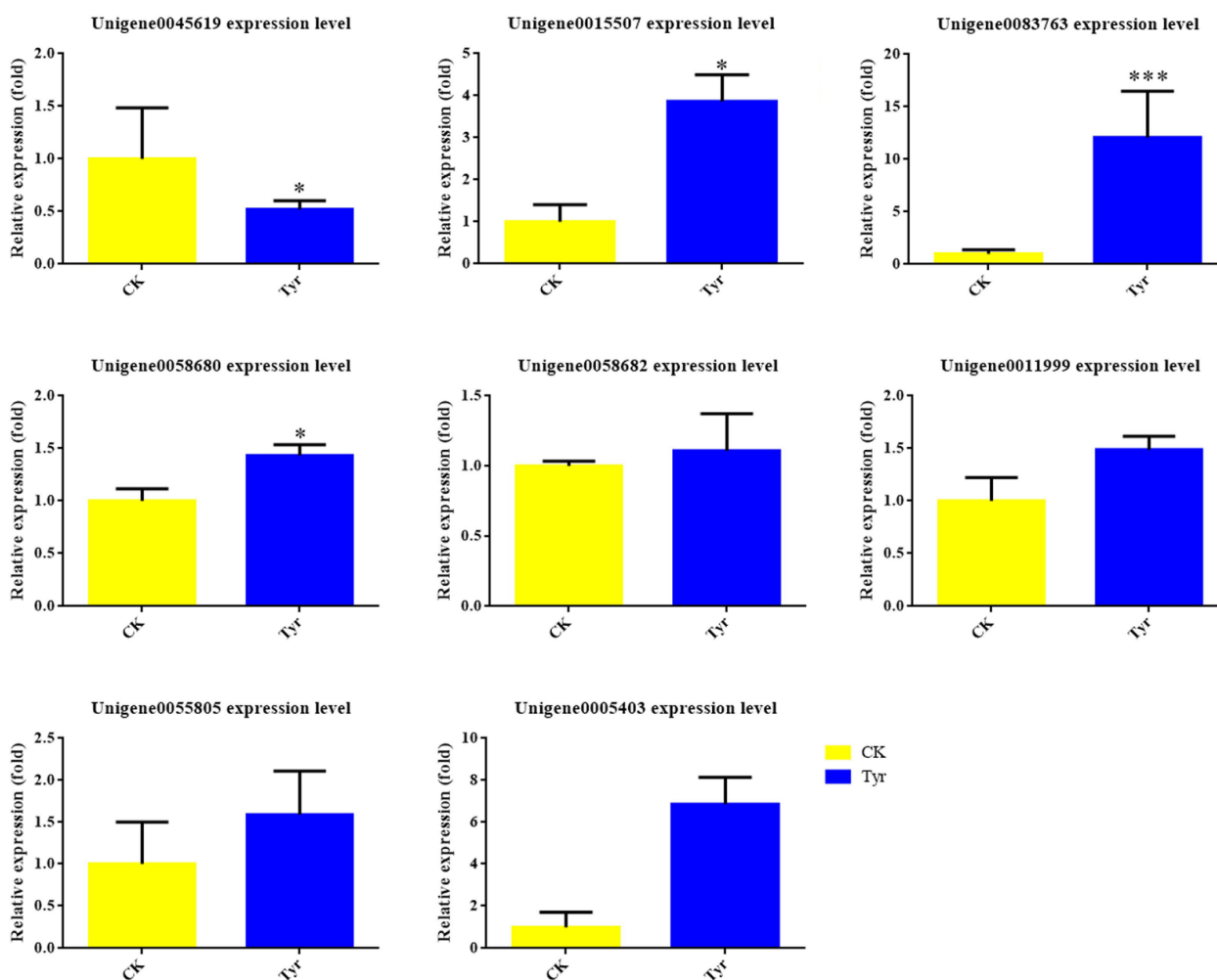


Fig. 5 The relative expression levels of anthocyanin biosynthesis and transcription factor genes in *Viola × wittrockiana* petals that received tyrosine (Tyr) or ddH₂O (CK) treatment. * $p \leq 0.05$, ** $p \leq 0.01$, *** $p \leq 0.001$.

treated areas based on $FDR < 0.05$ and $|\log_2FC| > 1$ (Table 2). This result suggested that the ABA content might be higher in the tyrosine-treated areas. We therefore analyzed ABA content and confirmed that it was significantly higher in the tyrosine-treated areas than in the H₂O-treated areas (Fig. 6).

We also analyzed differentially expressed bZIP TFs of pansy by building a phylogenetic tree with their sequences and those of all bZIP TFs from *Arabidopsis* (Supplemental Fig. S4). The upregulated unigene0087548 was highly homologous to the *Arabidopsis* TFs AT3G17609.2 and AT3G17609.3, which encode homologs of AtHY5, an important bZIP TF that binds to the promoter of the bZIP TF gene *ABA insensitive 5 (ABI5)* to activate ABA biosynthesis^[27].

Exogenous ABA upregulated the expression of anthocyanin biosynthesis genes

To determine whether ABA could activate anthocyanin-related genes in *Viola × wittrockiana*, we treated non-blotched areas of pansy petals with ABA and used ddH₂O as a control treatment. The treated petal areas were then collected for qRT-PCR analysis. As shown in Fig. 7, ABA treatment upregulated the expression levels of multiple anthocyanin biosynthesis genes, including *VwCHS*, *VwANS*, and *VwUGT*, as well as the TF genes *VwMYB12* and *VwHY5*.

DISCUSSION

Tyrosine promotes anthocyanin accumulation by upregulating *VwHCT*, *VwC3'H*, *VwCHS*, and *VwUGT*

Tyrosine has recently been shown to promote anthocyanin biosynthesis, and the molecular mechanism by which it induces anthocyanin biosynthesis in *Arabidopsis* has been investigated. Exogenous tyrosine is now known to induce anthocyanin biosynthesis and accumulation by upregulating anthocyanin biosynthesis-related genes, including *DFR*, *LODX*, and *UGT*^[18]. Tyrosine has also been found to promote the biosynthesis of flavonoids, the substrates of anthocyanin biosynthesis^[28]. These results suggest that tyrosine may serve as an efficient regulatory metabolite for anthocyanin biosynthesis.

In the present research, VIGS silencing of *VwCHS* and *VwANS* produced obvious fading of petal blotches, thus confirming that the VIGS protocol worked well in pansy. By contrast, VIGS silencing of *VwTYDC* induced pigment accumulation in pansy petals (Fig. 1), demonstrating that an increase in tyrosine promoted pigment biosynthesis in pansy. Moreover, the non-blotched parts of the petals showed some cyanic spots or stripes after tyrosine treatment (Fig. 2). Flowers were also significantly smaller after VIGS treatment. This phenomenon may reflect the ability of the VIGS technique to silence relevant

Anthocyanin biosynthesis in pansy

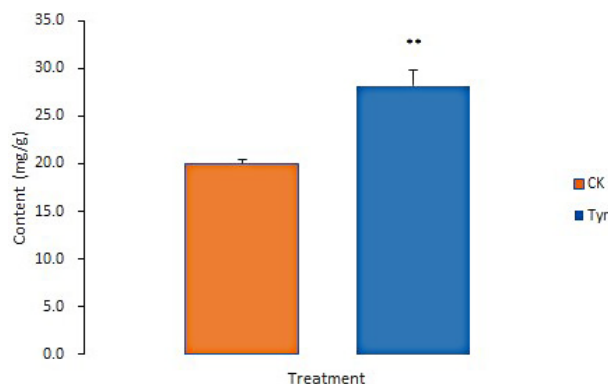


Fig. 6 ABA contents in *Viola × wittrockiana* from different treatment groups. ** $p \leq 0.01$. CK, ddH₂O treatment. Tyr, tyrosine treatment.

developmental genes, thereby affecting organ development; alternatively, wounding caused by the silencing treatment may have affected flower development (Fig. 2)^[29,30]. Anthocyanin metabolome analysis demonstrated that contents of cyanidin-3-O-glucoside and cyanidin-3-O-rutinoside were significantly enhanced by tyrosine treatment. Furthermore, delphinidin-3-O-rutinoside, delphinidin-3-O-rhamnoside, cyanidin-3,5-O-diglucoside, petunidin-3-O-rutinoside, peonidin-3,5-O-diglucoside, peonidin-3-O-galactoside, and pelargonidin-3-O-(coumaryl)-glucoside were detected in the tyrosine treatment but not the water control (Figs 3 & 4). Consistent with these findings, the transcriptome results indicated that *VwHCT*, *VwC3'H*, *VwCHS*, and *VwUGT* were upregulated in the tyrosine-treated areas. All these results suggest that tyrosine may promote anthocyanin accumulation by upregulating a number of anthocyanin biosynthesis-related genes.

Twenty-four different anthocyanins and related compounds were detected in the different samples (Fig. 4), among which almost all of the anthocyanins had been reported previously in *Viola*^[31]. Although the Tyr-1 data differed somewhat from those of Tyr-2 and Tyr-3, probably owing to difficulties in accurately sampling specific petal areas, cyanidin-3-O-rutinoside was the major enriched anthocyanin with the highest average content (5.098 ng/g) in tyrosine-treated areas, similar to the main anthocyanidins previously reported in the blotched areas of pansy petals^[1].

Tyrosine promotes anthocyanin biosynthesis via ABA synthesis in pansy

Previous studies have reported that endogenous or exogenous factors can induce anthocyanin accumulation through

Table 2. Differentially expressed genes related to ABA biosynthesis in *Viola × wittrockiana*.

Gene ID	Annotation	RPKM (Tyr treatment)	RPKM (H ₂ O treatment)	$\log_2 (T/CK)$	FDR	Up/Down
unigene0004917	<i>VwNCED</i>	2.20	1.03	1.10	0.00	Up
unigene0068071	<i>VwNCED</i>	2.41	0.56	2.10	7.18e-6	Up
unigene0068072	<i>VwNCED</i>	1.16	0.35	1.72	0.00	Up
unigene0082413	<i>VwABA2</i>	0.33	0.01	4.51	0.00	Up
unigene0073280	<i>VwAAO3</i>	8.81	4.28	1.04	2.46e-31	Up
unigene0017204	<i>VwCYP707A</i>	18.30	0.81	4.50	7.13e-212	Up
unigene0087548	<i>VwHY5</i>	0.63	0	9.29	0.01	Up

VwNCED, 9-cis-epoxycarotenoid dioxygenase; *VwABA2*, xanthoxin dehydrogenase 2; *VwAAO3*, abscisic-aldehyde oxidase; *VwCYP707A*, (+)-abscisic acid 8'-hydroxylase.

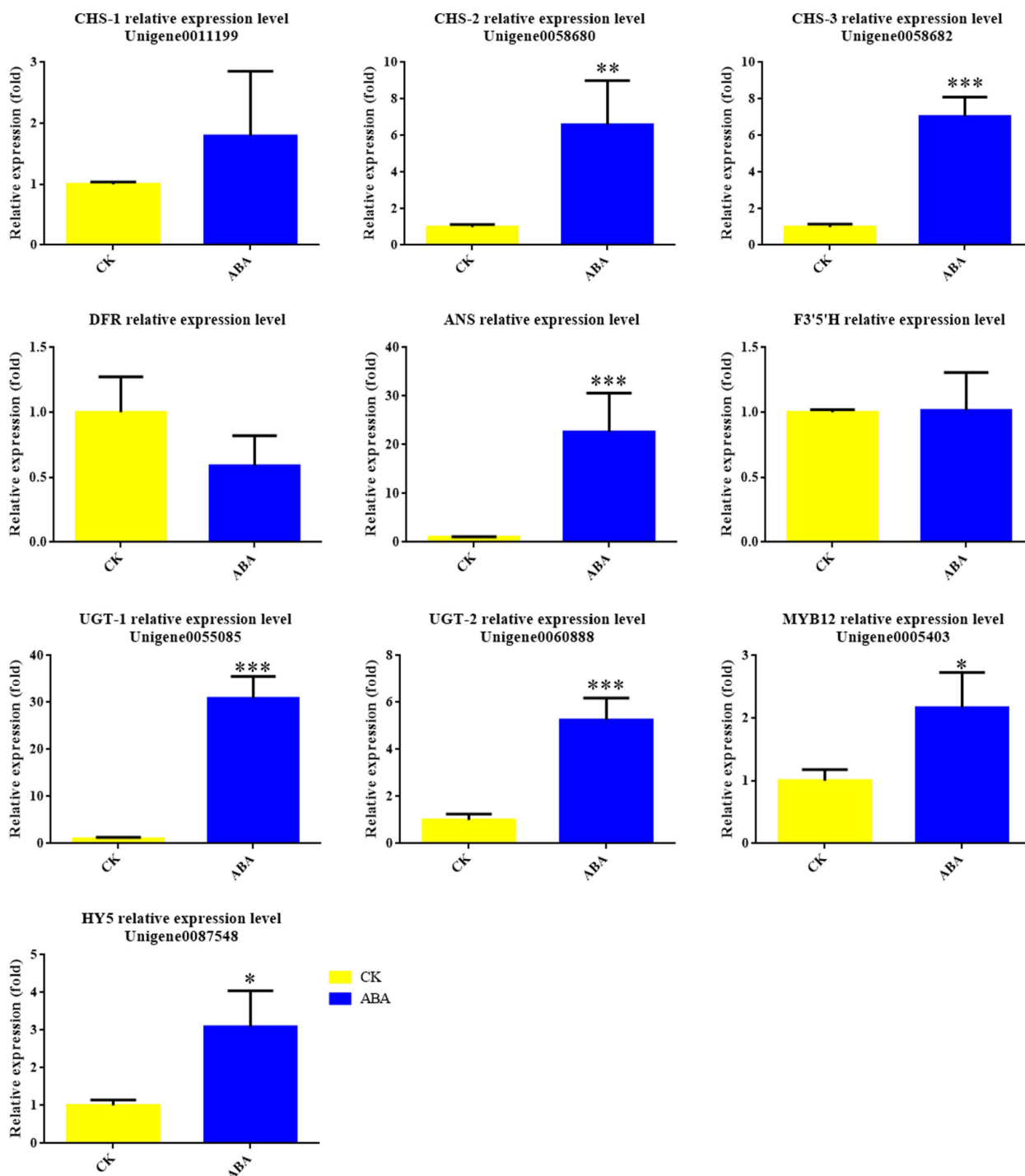


Fig. 7 Expression levels of anthocyanin biosynthesis genes and transcription factors in *Viola x wittrockiana* with and without ABA treatment. * $p \leq 0.05$, ** $p \leq 0.01$, *** $p \leq 0.001$.

ABA. In *Lycium*, for example, developmental cues transcriptionally activated *LbNCED1* and thereby enhanced accumulation of ABA. ABA then stimulated transcription of the MYB-bHLH-WD40 TF complex, which in turn upregulated the expression of structural genes in the flavonoid biosynthetic pathway, ultimately promoting anthocyanin production and fruit coloration^[32]. In bilberry (*Vaccinium myrtillus*), red light induced high expression of specific genes of anthocyanin biosynthesis and ABA signal perception and metabolism, including 9-cis-epoxycarotenoid dioxygenase (*NCED*), the ABA

receptor pyrabactin resistance-like (*PYL*), and an abscisic acid 8'-hydroxylase gene (*CYP707A*) that functions in ABA catabolism^[33]. ABA has been reported to promote anthocyanin accumulation by upregulating the expression of *CHS*, *ANS*, or *UGT*^[34]. In our research, exogenous tyrosine application significantly upregulated the expression of several ABA biosynthesis genes, including *VwNCED*, *VwABA2*, *VwAAO3*, and *VwCYP707A* (Table 2). At the same time, the concentration of ABA was significantly higher in the tyrosine-treated areas of pansy petals (Fig. 6). Moreover, ABA treatment also significantly

upregulated the expression of anthocyanin biosynthesis genes, including *VwCHS*, *VwANS*, and *VwUGT*, similar to the effect of tyrosine treatment on gene expression (Table 1). These results support a model in which tyrosine promotes anthocyanin biosynthesis via ABA accumulation in pansy petals.

Transcription factors may be important mediators of tyrosine-promoted anthocyanin biosynthesis

Anthocyanin biosynthesis genes are transcriptionally regulated by the MYB-bHLH-WD40 complex^[35]. In *Arabidopsis*, exogenous tyrosine upregulates the expression of MBW complex genes including *PAP1*, *PAP2*, *GL3*, *EGL3*, and *TTG1*^[18]. In this study, we found eight significantly upregulated MYB-like unigenes, among which unigene0005403 had high homology to *MYB12* from *Cicer arietinum*. Phylogenetic analysis with *Arabidopsis* MYBs also supported the hypothesis that unigene0005403 may have similar functions to *AtMYB12* (Supplemental Fig. S3), which upregulates early anthocyanin biosynthesis genes such as *CHS*, *CHI*, and *F3H*^[36]. These results suggest that unigene0005403 may also promote anthocyanin accumulation by upregulating anthocyanin biosynthesis genes. According to the transcriptome and qPCR data for *VwCHS*, *VwCHI*, and *VwF3H*, only *VwCHS* was significantly upregulated in response to tyrosine, and we thus speculate that unigene0005403 may act mainly on *VwCHS* in pansy.

bZIP TFs may also regulate anthocyanin biosynthesis by interacting synergistically with the MYBs^[37]. In *Arabidopsis*, *AtHY5* is a bZIP gene that can activate the expression of *MYB12/PFG1* and *MYB75/PAP1*^[38]. *HY5* is also known to activate the expression of *MYB12* and *MYB111*^[39], which are involved in the regulation of flavonol synthase^[40]. Moreover, *HY5* can respond to ABA by specifically binding to *ABI5* chromatin^[41]. In this research, unigene0087548, annotated as an *HY5*-like gene, and unigene0005403, annotated as an *MYB12* homolog, were both significantly upregulated in ABA-treated pansy petals (Fig. 7), suggesting that *HY5* may have responded to ABA treatment and interacted synergistically with *VwMYB12* to promote anthocyanin biosynthesis in pansy.

A proposed model of the promotion of anthocyanin biosynthesis by tyrosine in pansy

On the basis of our experimental results, we propose a working model of the promotion of anthocyanin biosynthesis by tyrosine treatment in pansy. Tyrosine treatment activates ABA production by upregulating *VwNCED*, *VwABA2*, *VwAAO3*, and *VwCYP707A*. Then the bZIP TF *VwHY5* responds to ABA accumulation and activates *VwMYB12* to upregulate *VwCHS* expression and then induce anthocyanin production in non-blotched areas of pansy petals (Fig. 8).

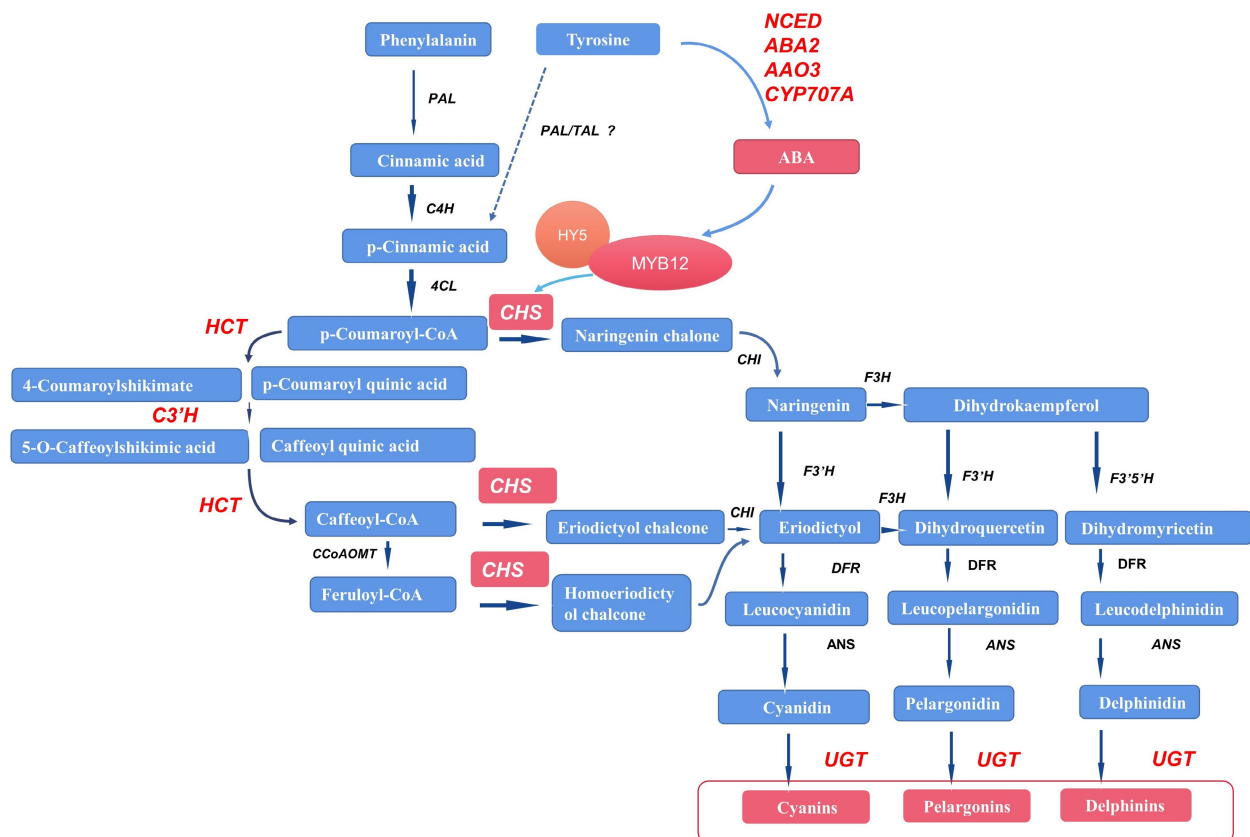


Fig. 8 Possible pathways by which tyrosine treatment may promote anthocyanin biosynthesis in *Viola × wittrockiana*. The red color represents upregulation of genes and metabolites. The dashed arrow represents the possible pathway. PAL/TAL indicates that PAL may function like TAL in pansy, although this remains to be verified. PAL: phenylalanine ammonia-lyase; TAL: tyrosine ammonia-lyase; C4H: cinnamate 4-hydroxylase; 4CL: 4-coumarate-CoA ligase; HCT: shikimate O-hydroxycinnamoyltransferase; C3'H: 5-O-(4-coumaroyl)-D-quinic acid 3'-monooxygenase; CHS: chalcone synthase; F3H: naringenin 3-dioxygenase; F3'H: flavonoid 3'-hydroxylase; F3'5'H: flavonoid 3',5'-hydroxylase; DFR: flavanone 4-reductase; ANS: anthocyanidin synthase; UGT: UDP glucuronosyltransferase, flavonoid 3-O-glycosyltransferase; CCoAOMT: caffeoyl-CoA O-methyltransferase; VwNCED: 9-cis-epoxycarotenoid dioxygenase; VwABA2: xanthoxin dehydrogenase; VwAAO3: abscisic-aldehyde oxidase; VwCYP707A: (+)-abscisic acid 8'-hydroxylase.

Anthocyanin biosynthesis in pansy

Another possible pathway is that exogenous tyrosine promotes the production of p-coumaric acid, which then leads to increased anthocyanin content. Tyrosine is known to give rise to p-coumaric acid through the catalysis of tyrosine ammonia-lyase (TAL); p-coumaric acid is then acted upon by 4-coumarate-CoA ligase (4CL) to form p-coumaroyl CoA, the main precursor of the anthocyanin biosynthesis pathway. When the content of tyrosine increases, p-coumaric acid production may be upregulated, thus promoting anthocyanin biosynthesis. However, no unigenes in the *Viola × wittrockiana* transcriptome were annotated as TAL in the present study. We speculate that phenylalanine ammonia-lyase of pansy (VwPAL) may have the same function as TAL, as PAL has been shown to function like TAL in some other plants^[42]. However, more experiments are needed to verify this hypothesis.

ACKNOWLEDGMENTS

This research was supported by the National Natural Science Foundation of China (Grant No. 32160719, 32060365 and 31760590), the Natural Science Foundation of Guizhou Province (No. ZK [2022] 095), and the Cultivation Research Program of Guizhou University (No. [2018] 5781).

Conflict of interest

The authors declare that they have no conflict of interest.

Supplementary Information accompanies this paper at (<https://www.maxapress.com/article/doi/10.48130/TP-2022-0009>)

Dates

Received 7 September 2022; Accepted 2 November 2022; Published online 29 November 2022

REFERENCES

- Li Q, Wang J, Sun H, Shang X. 2014. Flower color patterning in pansy (*Viola × wittrockiana* Gams.) is caused by the differential expression of three genes from the anthocyanin pathway in acyanic and cyanic flower areas. *Plant Physiology and Biochemistry* 84:134–41
- Endo T. 1959. Biochemical and Genetical Investigations of Flower Color in Swiss Giant Pansy, *Viola × Wittrockiana* Gams. III. *The Japanese journal of genetics* 34:116–24
- Henry-Kirk RA, Plunkett B, Hall M, McGhie T, Allan AC, et al. 2018. Solar UV light regulates flavonoid metabolism in apple (*Malus × domestica*). *Plant, Cell & Environment* 41:675–88
- Hsu CC, Chen HH. 2017. *Flower Color and Pigmentation Patterns in Phalaenopsis Orchids: Orchid Biotechnology III*. pp: 393–420
- Winkel-Shirley B. 2001. Flavonoid biosynthesis. A colorful model for genetics, biochemistry, cell biology, and biotechnology. *Plant Physiology* 126:485–493
- Li L, Ye J, Li H, Shi Q. 2020. Characterization of Metabolites and Transcripts Involved in Flower Pigmentation in *Primula vulgaris*. *Frontiers in Plant Science* 11:572517
- Gu Z, Zhu J, Hao Q, Yuan YW, Duan YW, et al. 2019. A novel R2R3-MYB transcription factor contributes to petal blotch formation by regulating organ-specific expression of *PsCHS* in tree peony (*Paeonia suffruticosa*). *Plant and Cell Physiology* 60:599–611
- Stracke R, Ishihara H, Huep G, Barsch A, Mehrrens F, et al. 2007. Differential regulation of closely related R2R3-MYB transcription factors controls flavonol accumulation in different parts of the *Arabidopsis thaliana* seedling. *The Plant Journal* 50:660–77
- Shan X, Zhang Y, Peng W, Wang Z, Xie D. 2009. Molecular mechanism for jasmonate-induction of anthocyanin accumulation in *Arabidopsis*. *Journal of Experimental Botany* 60:3849–60
- Deikman J, Hammer PE. 1995. Induction of Anthocyanin Accumulation by Cytokinins in *Arabidopsis thaliana*. *Plant Physiology* 108:47–57
- El-Kereamy A, Chervin C, Roustan JP, Cheynier V, Souquet JM, et al. 2010. Exogenous ethylene stimulates the long-term expression of genes related to anthocyanin biosynthesis in grape berries. *Physiologia Plantarum* 119:175–82
- Peng Z, Han C, Yuan L, Zhang K, Huang H, et al. 2011. Brassinosteroid enhances jasmonate-induced anthocyanin accumulation in *Arabidopsis* seedlings. *Journal of Integrative Plant Biology* 53:632–640
- Loreti E, Povero G, Novi G, Solfanelli C, Alpi A, et al. 2008. Gibberellins, jasmonate and abscisic acid modulate the sucrose-induced expression of anthocyanin biosynthetic genes in *Arabidopsis*. *New Phytologist* 179:1004–16
- Li G, Zhao J, Qin B, Yin Y, An W, et al. 2019. ABA mediates development-dependent anthocyanin biosynthesis and fruit coloration in *Lycium* plants. *BMC Plant Biology* 19:317
- An J, Yao J, Xu R, You C, Wang X, et al. 2018. Apple bZIP transcription factor MdbZIP44 regulates abscisic acid-promoted anthocyanin accumulation. *Plant, Cell & Environment* 41:2678–92
- Polturak G, Grossman N, Vela-Corcia D, Dong Y, Nudel A, et al. 2017. Engineered gray mold resistance, antioxidant capacity, and pigmentation in betalain-producing crops and ornamentals. *PNAS* 114:9062–67
- Zha J, Koffas MAG. 2017. Production of anthocyanins in metabolically engineered microorganisms: Current status and perspectives. *Synthetic and Systems Biotechnology* 2:259–66
- Zhou Z, Zhi T, Liu Y, Chen Y, Ren C. 2014. Tyrosine Induces Anthocyanin Biosynthesis in *Arabidopsis thaliana*. *American Journal of Plant Sciences* 5:328–31
- Yang W, Peng T, Li T, Cen J, Wang J. 2018. Tyramine and tyrosine decarboxylase gene contributes to the formation of cyanic blotches in the petals of pansy (*Viola × wittrockiana*). *Plant Physiology and Biochemistry* 127:269–75
- Li R, Yu C, Li Y, Lam TW, Yiu SM, et al. 2009. SOAP2: an improved ultrafast tool for short read alignment. *Bioinformatics* 25:1966–67
- Grabherr MG, Haas BJ, Yassour M, Levin JZ, Thompson DA, et al. 2011. Full-length transcriptome assembly from RNA-Seq data without a reference genome. *Nature Biotechnology* 29:644–52
- Mortazavi A, Williams BA, McCue K, Schaeffer L, Wold B. 2008. Mapping and quantifying mammalian transcriptomes by RNA-Seq. *Nature methods* 5:621–28
- Iseli C, Jongeneel CV, Bucher P. 1999. ESTScan: a program for detecting, evaluating, and reconstructing potential coding regions in EST sequences. *Proceedings of International Conference on Intelligent Systems for Molecular Biology, Heidelberg, 1999*. pp: 138–48.
- Conesa A, Götz S, García-Gómez JM, Terol J, Talón M, et al. 2005. Blast2GO: a universal tool for annotation, visualization and analysis in functional genomics research. *Bioinformatics* 21:3674–76
- Ye J, Fang L, Zheng H, Zhang Y, Chen J, et al. 2006. WEGO: a web tool for plotting GO annotations. *Nucleic Acids Research* 34:W293–W297
- Willems E, Leyns L, Vandesompele J. 2008. Standardization of real-time PCR gene expression data from independent biological replicates. *Analytical Biochemistry* 379:127–29
- Chen H, Zhang J, Neff MM, Hong SW, Zhang H, et al. 2008. Integration of light and abscisic acid signaling during seed germination and early seedling development. *PNAS* 105:4495–500
- Ma Q, Li H, Zou Z, Arkorful E, Lv Q, et al. 2018. Transcriptomic analyses identify albino-associated genes of a novel albino tea germplasm 'Huabai 1'. *Horticulture Research* 5:54

29. Hsieh MH, Pan ZJ, Lai PH, Lu HC, Yeh HH, et al. 2013. Virus-induced gene silencing unravels multiple transcription factors involved in floral growth and development in Phalaenopsis orchids. *Journal of Experimental Botany* 64:3869–84
30. Chen Z. 2017. *Establishment of Virus-induced Gene Silencing (VIGS) in Gerbera jamesonii 'Hualong' and Its Application in Gene Functional Analysis*. Thesis. South China Agricultural University, China. pp. 61–62
31. Zhang J, Wang LS, Gao JM, Xu YJ, Li LF, et al. 2012. Rapid separation and identification of anthocyanins from flowers of *Viola yedoensis* and *V. prionantha* by high-performance liquid chromatography–photodiode array detection–electrospray ionisation mass spectrometry. *Phytochemical Analysis* 23:16–22
32. Li G, Qin B, Li S, Yin Y, Zhao J, et al. 2020. LbNR-Derived Nitric Oxide Delays *Lycium* Fruit Coloration by Transcriptionally Modifying Flavonoid Biosynthetic Pathway. *Frontiers in Plant Science* 11:1215
33. Samkumar A, Jones D, Karppinen K, Dare AP, Sipari N, et al. 2021. Red and blue light treatments of ripening bilberry fruits reveal differences in signalling through abscisic acid-regulated anthocyanin biosynthesis. *Plant Cell and Environment* 44:3227–45
34. Oh HD, Yu DJ, Chung SW, Chea S, Lee HJ. 2018. Abscisic acid stimulates anthocyanin accumulation in 'Jersey' highbush blueberry fruits during ripening. *Food Chemistry* 244:403–7
35. Xu W, Dubos C, Lepiniec L. 2015. Transcriptional control of flavonoid biosynthesis by MYB-bHLH-WDR complexes. *Trends in Plant Science* 20:176–85
36. Han M, Yang C, Zhou J, Zhu J, Meng J, et al. 2020. Analysis of flavonoids and anthocyanin biosynthesis-related genes expression reveals the mechanism of petal color fading of *Malus hupehensis* (Rosaceae). *Brazilian Journal of Botany* 43:81–89
37. Hartmann U, Sagasser M, Mehrtens F, Stracke R, Weisshaar B. 2005. Differential combinatorial interactions of cis-acting elements recognized by R2R3-MYB, BZIP, and BHLH factors control light-responsive and tissue-specific activation of phenylpropanoid biosynthesis genes. *Plant Molecular Biology* 57:155–71
38. Shin DH, Choi M, Kim K, Bang G, Cho M, et al. 2013. *HY5* regulates anthocyanin biosynthesis by inducing the transcriptional activation of the MYB75/PAP1 transcription factor in *Arabidopsis*. *FEBS Letters* 587:1543–47
39. Berli FJ. 2010. Abscisic acid is involved in the response of grape (*Vitis vinifera* L.) cv. Malbec leaf tissues to ultraviolet-B radiation by enhancing ultraviolet-absorbing compounds, antioxidant enzymes and membrane sterols. *Plant, Cell & Environment* 33:1057
40. Brunetti C, Sebastiani F, Tattini M. 2019. Review: ABA, flavonols, and the evolvability of land plants. *Plant Science* 280:448–54
41. Fujita Y, Fujita M, Shinozaki K, Yamaguchi-Shinozaki K. 2011. ABA-mediated transcriptional regulation in response to osmotic stress in plants. *Journal of Plant Research* 124:509–25
42. Khan W, Prithiviraj B, Smith DL. 2003. Chitosan and chitin oligomers increase phenylalanine ammonia-lyase and tyrosine ammonia-lyase activities in soybean leaves. *Journal of Plant Physiology* 160:859–63



Copyright: © 2022 by the author(s). Published by Maximum Academic Press on behalf of Hainan University. This article is an open access article distributed under Creative Commons Attribution License (CC BY 4.0), visit <https://creativecommons.org/licenses/by/4.0/>.